Investigation of Turbulent Spray Disintegration Characteristics Depending on the Nozzle Configuration

Sam Goo Lee*
Research Fellow, Automobile High Technology Research Institute, Chonbuk National University, Chonbuk 561-756, Korea
Kyu Keun Song, Byung Joon Rho
Prof., Faculty of Mechanical & Aerospace Engrg., AHTRI, Chonbuk National University, Chonbuk 561-756, Korea

The experimental measurements were carried out to examine turbulent disintegration characteristics ejecting from a counter-flowing internal mixing pneumatic nozzle under variable conditions of swirl angles and air pressures. The air injection pressure was varied from 60 kPa to 180 kPa and four counter-flowing internal mixing nozzles with axi-symmetric tangential-drilled holes at swirl angle of 15°, 30°, 45°, and 60° to the central axis have been specially designed. The experimental results were quantitatively analyzed, focusing mainly on the comparison of turbulent atomization characteristics issuing from an internal mixing swirl nozzle. To illustrate the swirl phenomena, the distributions of mean velocities, turbulence intensities, volume flux, and SMD (Sauter Mean Diameter, or D_{32}) were comparatively analyzed.

Key Words : SMD (Sauter Mean Diameter), PDPA (Phase Doppler Particle Analyzer), ALR (Air to Liquid Mass Ratio), Counter Swirl Atomizer

Nomenclature

ALR : Air to liquid mass ratio
d_o : Final discharge orifice diameter
d_p : Diameter of passages for fluids
D_{32} : Sauter mean diameter
D_s : Swirl chamber diameter
l_{ap} : Length of air passages
l_o : Length of final discharge orifice
l_s : Length of swirl chamber
l_{wp} : Length of liquid passages
R : Radial distances
u'_{rms} : Root mean square in axial velocity
U_m : Maximum axial velocity at the centerline
U : Axial velocity
V : Radial velocity
W : Tangential velocity
Z : Axial distances from the nozzle tip
θ_s : Swirl angle of the inlet passages for fluids

* Corresponding Author,
E-mail : sglee39@hotmail.com
TEL : +82-63-277-7308; **FAX** : +82-63-270-2388
Research Fellow, Automobile High Technology Research Institute, Chonbuk National University, Chonbuk 561-756, Korea. (Manuscript **Received** October 6, 2001; **Revised** February 18, 2002)

1. Introduction

The disintegration mechanism in twin fluid atomizers is still being investigated in order to characterize the optimum models. Regarding this consideration, one of the prerequisites for good atomization is to get a high momentum of droplets, caused by mutual interactions. The purpose of breaking up the liquid into multitudinous small droplets is to increase the liquid surface area and to improve disintegration. Therefore, the atomization in two-phase flows is most effectively achieved by generating a high relative velocity between the liquid jet and surrounding air. Also, air/liquid mass flow ratio (ALR) and geometric configuration of the nozzle are known as important parameters affecting the mixing pro-

cess. In this article, nozzle configurations were varied to increase mixing within the passages of twin fluids.

A large number of literatures have been reported on disintegration process, and some improved results were obtained. Mansour et al. (1990) and was Lee et al. (2001) showed that the SMD was progressively reduced as the air/liquid mass ratio is increased. Kennedy (1986) found that the SMD was varied linearly with the liquid surface tension while the influence of the viscosity was minimized. Lee (2000-2001) showed that the smaller droplets were inwardly entrained from the spray boundary. Mullinger and Chigier (1974) showed the advantage for the internal mixing atomizers that the atomizing fluid could generally be supplied to the mixing region at a higher pressure than the external mixing type.

The aim in this experimental investigation was intended to describe the turbulent mixing flow and disintegration characteristics issuing from the internal mixing counterflowing two-phase jets.

2. Experimental Methodology

2.1 Nozzle

The body of prototype nozzle for generating a counter-flowing spray is fabricated of brass. The nozzle configuration used to establish counter-flowing mixing in an axi-symmetric jet is schematically shown in Fig. 1. The discharge orifice diameter (d_o) is 2mm, swirl chamber diameter (D_s) is 9mm, and the length/diameter ratio of the discharge orifice is 0.65 ($l_o \fallingdotseq 1.3$mm). The working fluids are flowed through the tangential ports that cause the liquid and the air an angular velocity, interacted together in a mixing chamber and injected into the quiescent ambient air at room temperature.

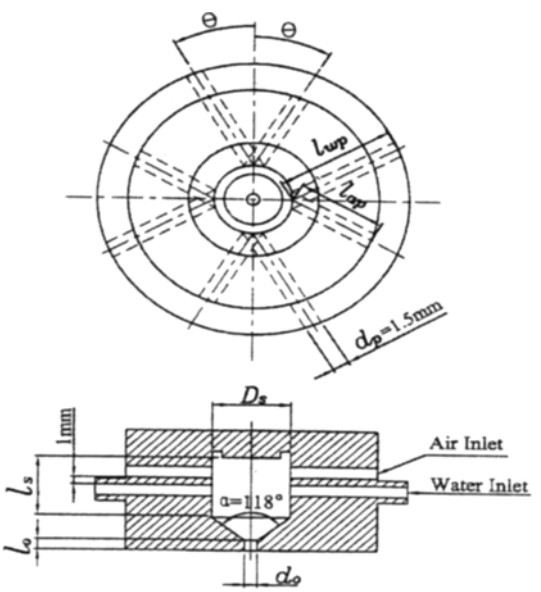

Fig. 1 Geometric nozzle configuration used for the counter swirl experiment

2.2 Experimental set-up

The experimental apparatus is shown schematically in Fig. 2. Continuous and steady atomizing water and the pulsation-free air are supplied to the mixing chamber from a pressurized storage tank. Working fluids are properly filtered and regulated. A number of valves, pressure gauges, and flow meters are located in a nozzle feed line to provide the desired operating conditions. Experiments are conducted while the liquid flow rate is kept constant at 7.95g/s, and the air pressures are gradually increased from 20kPa to 200 kPa, thus, air to liquid mass flow ratio varied from 0.054 to 0.132. Since the liquid velocity is maintained constant, an increase in air velocity

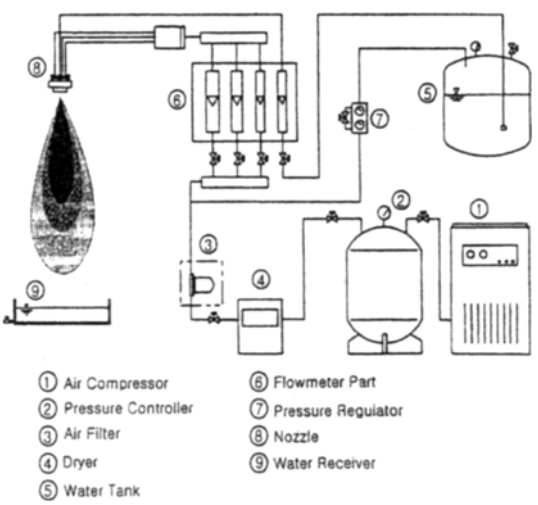

Fig. 2 Schematic set up for the experimental apparatus

contributes to an increase of air to liquid relative velocity, consequently imposing higher aerodynamic force on the liquid.

2.3 Diagnostics

A Phase Doppler Particle Anemometer is installed to specify spray flows. It provides information on individual particle size between 1μm and 250μm passing through the measurement volume in this investigation. The focal lengths of transmitting and receiving optics are 400mm and 500mm, respectively. The photomultiplier detector voltage of 1400V is optimized to provide the greatest sensitivity, and 45° of scattering is made in the forward direction. Also, a bragg cell is used to shift the frequency of one beam by 40MHz to provide directional sensitivity. The data acceptance rate in this experiment is too low for distances less than 20mm from the nozzle exit. Reasons for the low S/N ratio is usually attributed to the presence of non-spherical particles in the PDPA probe volume. Because the PDPA works on the principle of light scattering by spherical particles, signals obtained from the non-spherical particles will automatically be rejected by the instrument. Data acceptance rate varied from 60% to 98% depending on the experimental conditions and the location of the probe in relation to the spray geometry. The spray was checked for axial symmetry in a few selected cases across the entire spray, but no significant asymmetry was noticed.

2.4 Coordinates

Radial profiles of a geometric sequence space at each measurement locations were obtained at several axial stations located up to $Z/d_o=60$ downstream from the nozzle exit. The coordinate Z corresponds to the streamwise drops, moved in the downstream direction at the nozzle exit and y signifies radial outward motion. The measurement volume can be positioned easily at various stations without moving the diagnostic systems in three orthogonal directions by using a computer controlled traversing system that permits positioning to within 0.02mm.

2.5 Data Acquisition

The droplet quantities were calculated by collecting 10,000 sample data at each point. While the sampling time depends on the local number density of droplets, 10 seconds was set as an upper limit to record meaningful data for the analysis. Precautions for the accurate measurement were taken to avoid possible sources of error during the experiments such as mistracking the particles, nozzle vibrations, and reading of the flow meters, etc. The mists of small droplets were also discharged to an exhaust system to prevent splashing. To establish repeatability of the data received, each profile was measured at least twice at different times.

3. Results and Discussion

Figure 3 indicates a characteristic sequence of the liquid jet structure based on photographs at different swirl conditions. The liquid from the nozzle emerges as less disintegrated jet at lower ALR as shown in Fig. 3(a). The tangential swirling motion at the exit orifice is noticeable as the swirl angle increases. At the beginning stage,

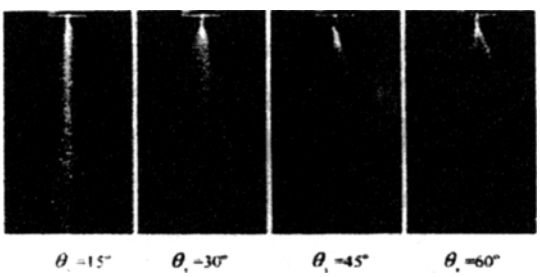

Fig. 3(a) Photographic visualization for the lower ALR

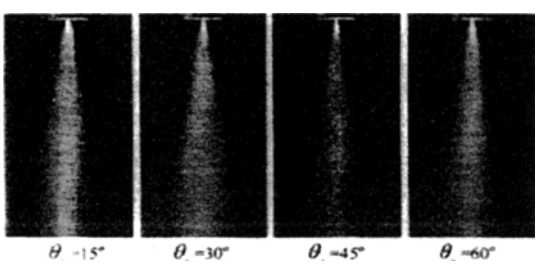

Fig. 3(b) Photographic visualization for the higher ALR

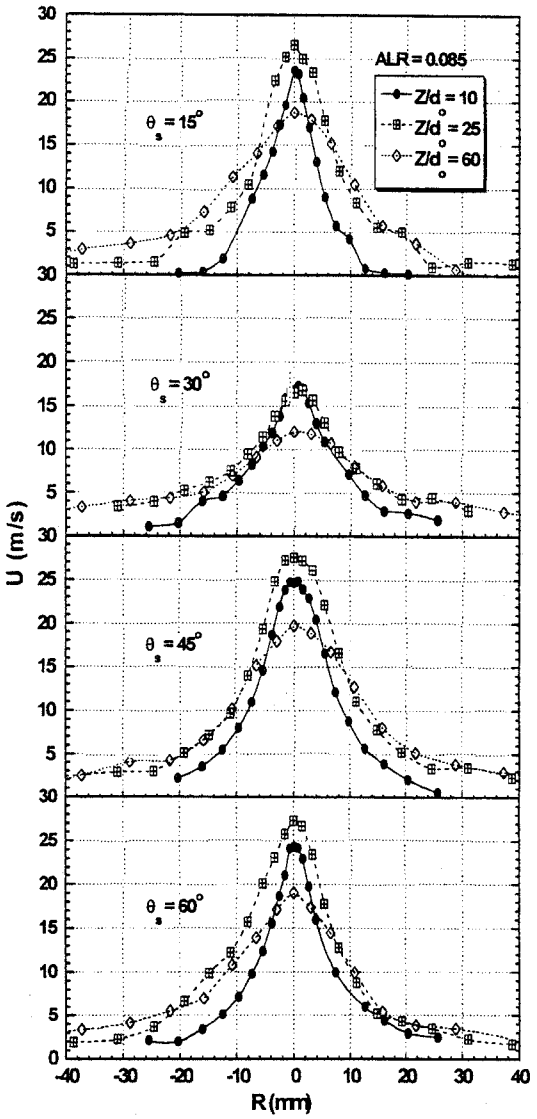

Fig. 4 Distributions of axial mean velocity for different swirl angles measured at three axial downstream locations

the swirl impacts can be seen evidently, and the liquid emerges as a hollow cone near the tip as shown in Fig. 3(a). But, twisting conical shapes appear and grow at some distances away from the nozzle tip, indicating the typical aspect of the swirl atomizer. Thus, it can explain the breakup process, corresponding to the contraction due to the drag, and dispersion by the swirl, which finally cause the discontinuities of droplets issuing from the atomizer. That is, the twisting bubble shape of converging sheet abruptly diverges, leading to disintegration into ligaments and large drops even for the lower ALR case.

On the other hand, with the higher air mass ratio as shown in Fig. 3(b), no perturbations appear and the number of clusters are remarkably reduced compared to Fig. 3(a). Also, the breakup region suddenly moves back close to the nozzle by the rise in air mass ratio and the twisting onion shape can't be observed any longer. Fig. 3(b) showed an increased air mass flow rate by a factor of three relative to the flows in Fig. 3(a). It indicates an increase of radial growth rate so that the disintegration aspects are more readily observed. Accordingly, an increase in the air mass flow rate results in an increase for the spray angle and the smaller droplets.

Figure 4 shows the radial profiles of mean axial velocity at three axial positions under the different swirl conditions. It is considered that the droplets emanating from the nozzle exhibit an explicit similarity of spray transport regardless of different swirl angles. It also reveals the droplet in the central parts propagate farther downstream due to easy access of atomizing air, whereas the accelerations at the spray boundary are discernibly less by loss of axial momentum and surrounding drag. This is attributed to the fact that the spray behavior near the axis seems to have higher momentum and is subject to higher acceleration even though its geometric conditions are dissimilar. Although the distributions are seen to be geometrically symmetric about the spray axis, and they have nearly qualitatively consistent value when compared, the effects of swirl inclination for θ_s=30° are quite visible. The distributions for the case of θ_s=30° are much smaller even in the central parts. This difference in velocity variation can be possibly substantiated by photographic observation in Fig. 3. The spray dispersion is wider than those of other angles. This growth rate because of characteristic strong swirl in the case of θ_s=30° hinders the axial downward propagation.

The distributions in Figs. 5-6 indicate another significant characteristic feature of swirling

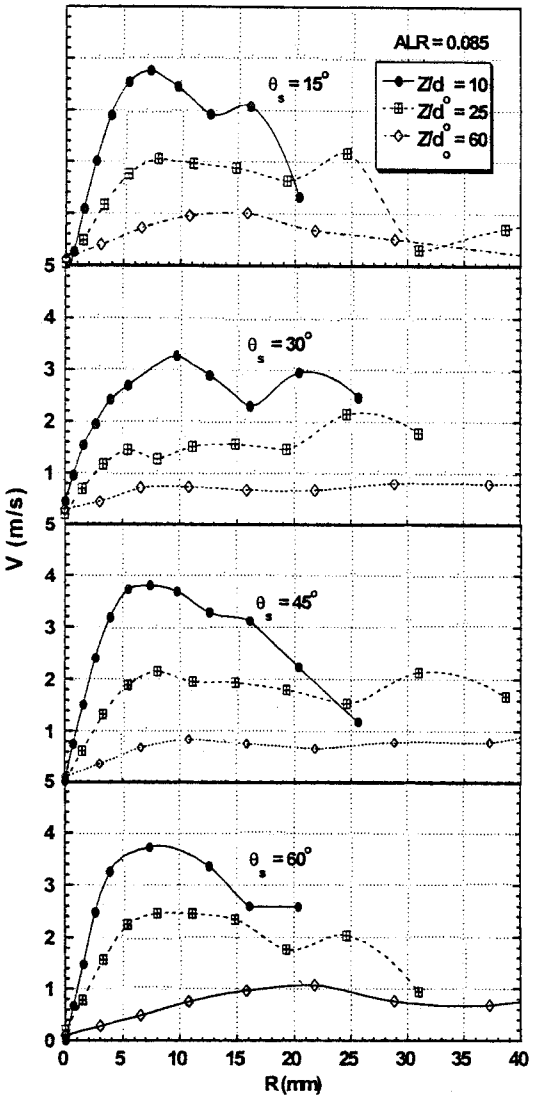

Fig. 5 Distributions of radial mean velocity for different swirl angles measured at three axial downstream locations

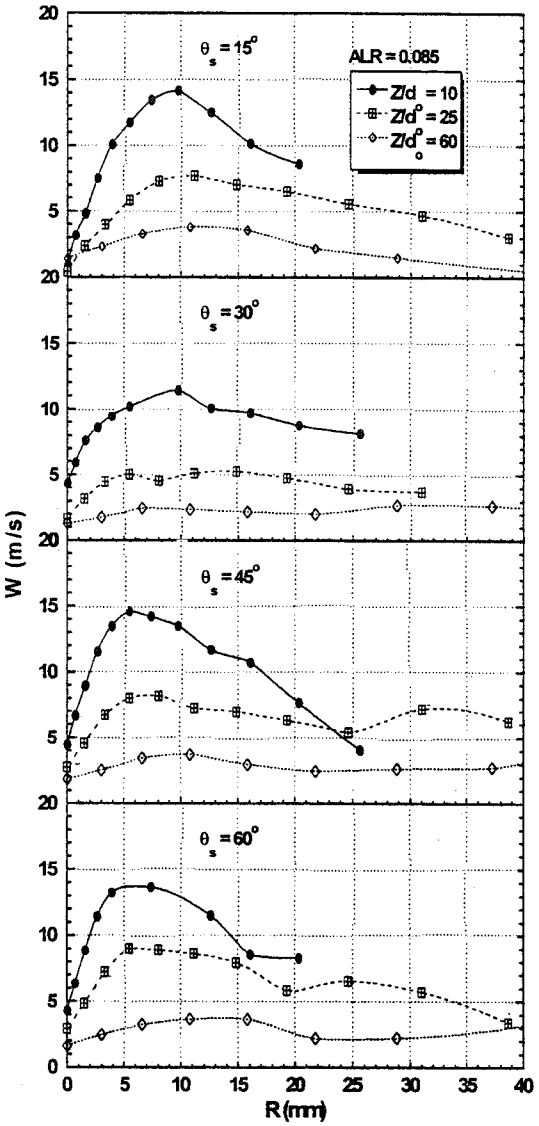

Fig. 6 Distributions of tangential mean velocity for different swirl angles measured at three axial downstream locations

atomizer. The radial and tangential velocities in the center show a minimum value, which comprise the maximum in axial velocity as shown in Fig. 4. This is mainly because the effects of downward axial penetration tend to subside the growth rate. But the spray trajectory in radial and tangential components exhibits a progressive dispersion to the outer regions from zero in the axis, shifting the location of maximum velocity at all conditions. After reaching a maximum value, the velocities are sluggishly decreased. Even though the spray patterns are similar, big differences in velocity are apparent between two components. The spray transport is quite comparable as indicated by the turbulence intensities in Fig. 7. The droplets located in the center and the downstream regions have the maximum axial turbulence intensity in all conditions, while having comparatively smaller values toward the boun-

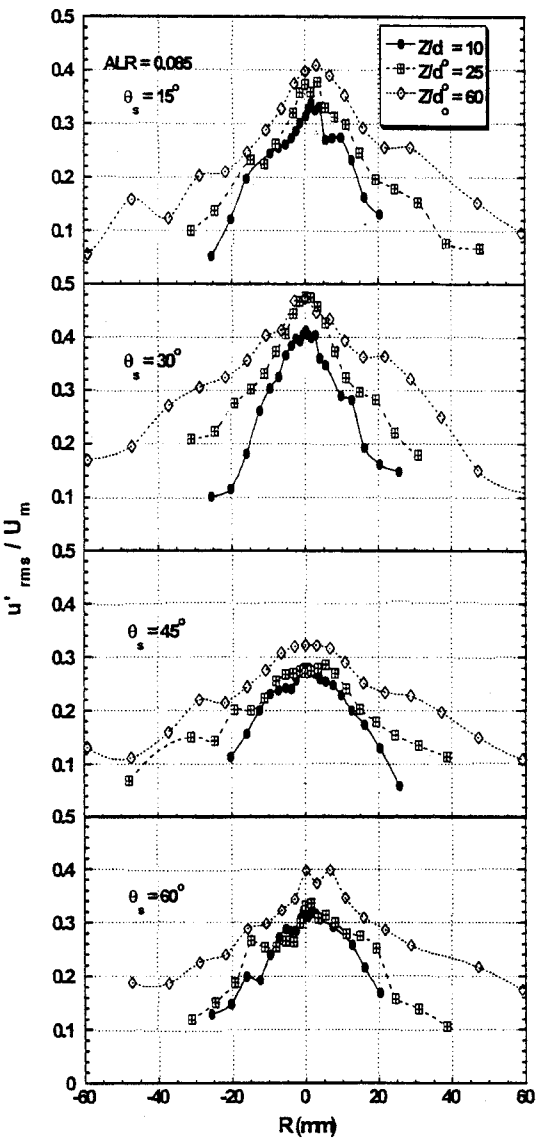

Fig. 7 Distributions of turbulence intensities for different swirl angles measured at three axial downstream locations

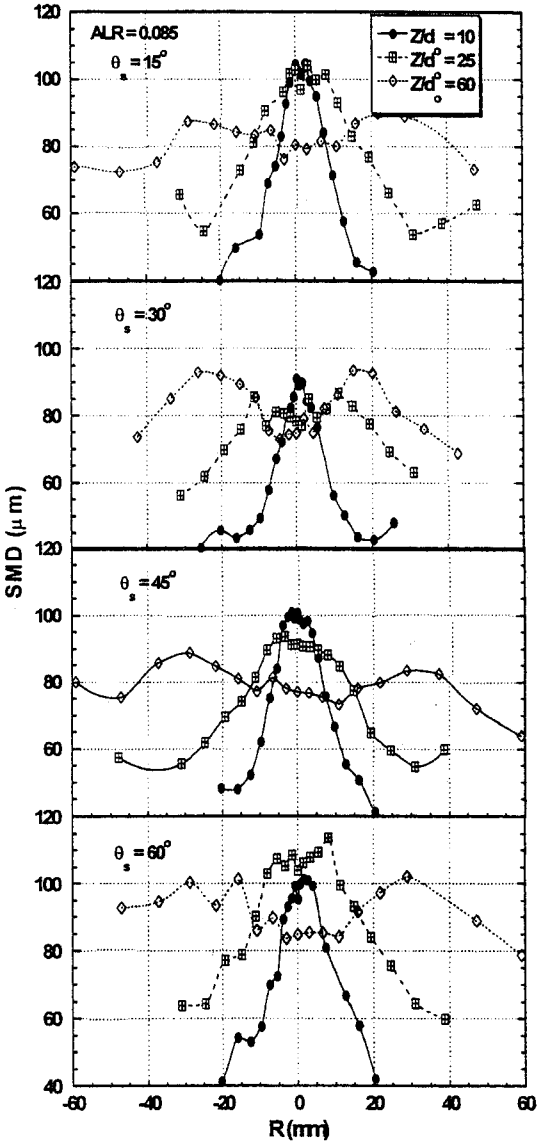

Fig. 8 Distributions of sauter mean diameter different swirl angles measured at three axial downstream locations

dary and upstream locations. This explains that the sprays acquire large velocity fluctuations for all the cases in the center as an acceleration stage. An interesting result can be drawn from this. Even with a strong axial momentum close to the nozzle exit, the downstream turbulence intensities are much higher than the upstream. This is presumably because of the non-spherical particles or less disintegrated droplets at upstream. As the sprays are in an evolving stage, it is considered that the atomization of the droplets can be brisk at downstream region, which is one of the characteristics in counter-swirling internal mixing nozzle.

Figure 8 shows the SMD variation measured at different swirling conditions. At upstream regions, the droplets even in the center part are typically larger than that of downstream. As

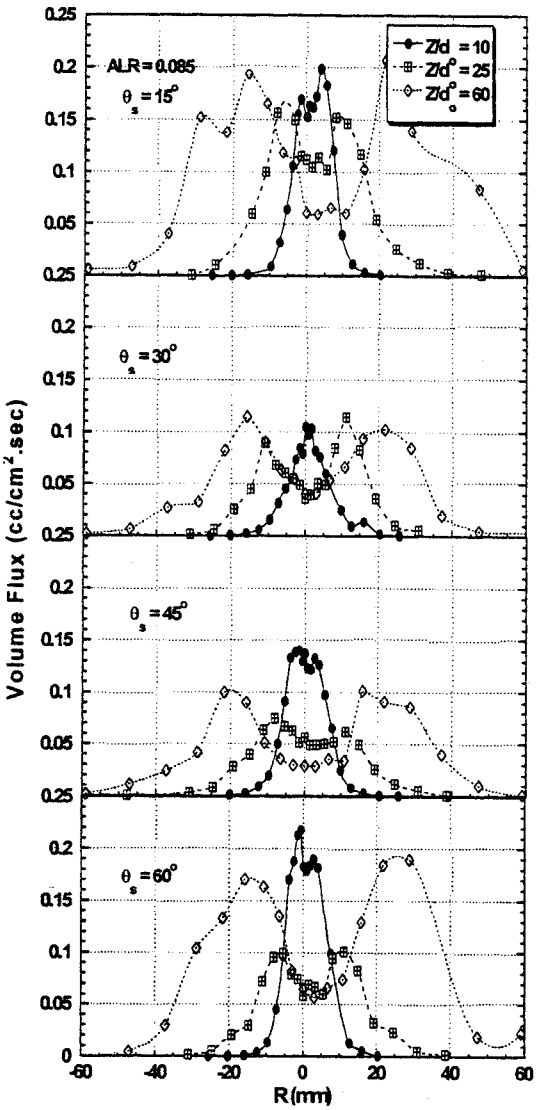

Fig. 9 Distributions of volume flux for different swirl angles measured at three axial downstream locations

shown for all the cases, the initial increase in SMD is partly due to the possibility of coalescence from the less atomized droplets in spite of strong penetration, showing that SMD decreases from approximately 80–110μm at upstream to 60–90μm at downstream. Contrast to the upstream transport, however, the SMD in the spray periphery gradually increases, which might be explained by entrainment of the small droplets from the outer part to the central region. This result was reported in the previous research that the smaller droplets in the peripheral region tended to be entrained inwardly and the larger ones inclined to remain in that region. The smaller diameters at upstream are less abundant in the center region, and the presence of relatively smaller ones near the boundary is ascribed to the distinctive feature in this swirl nozzle. Also, it is interesting to observe that a variation in SMD for θ_s=30° is the lowest among these nozzles. It could be substantiated by the photographic pattern as shown in Fig. 3. It is also confirmed that the wider radial growth rate restrains the axial penetration and the brisk turbulence fluctuation means better atomization in the spray field.

Distributions of volume flux in Fig. 9 show a good coincidence with SMD variation as shown in Fig. 8. At upstream, the high rates of volume fluxes are existed on the axis, but the trend for the downstream is quite different. The examination of these profiles provides a discernible difference for θ_s=30°. The volume fluxes in this angle are evidently smaller than those of the other swirl angles, indicating more positive influence on the improved atomization. The highest volume flux near the spray boundary at all conditions means the dense concentration of comparatively higher number density with larger drop diameters.

4. Conclusions

From the experimental analysis for the internal mixing swirl spray, the following conclusions can be drawn.

Photographic visualization shows that no twisting conical perturbations for the higher ALR can be seen as they do for the case of the lower ALR. It indicates that an increase of ALR results in an expansion of radial growth rate, reducing the number of clusters. Although the axial velocity distributions for θ_s=30° are much smaller even in the central parts, it can explain the positive swirl effects for disintegration. Especially, the turbulence intensities for the case of θ_s=30° are higher than the other cases at every axial locations, explaining brisk velocity fluctuations with strong swirl momentum. As indicated for all

the variations in SMD and volume flux, the initial increase is due to the possibility of coalescence of the less disintegrated droplets with dense concentration. Thus, it can be inferred that the nozzle configuration with a swirl of 30° to the central axis is recommendable for better disintegration compared to the other ones.

Acknowledgement

This work was supported by the grant of Post-doc program, Chonbuk National University, Korea

References

Kennedy, J. B., 1986, "High number SMD Correlations for Pressure Atomizers," *Journal of Engrg., for Gas Turbines and Power*. pp. 191~195.

Lee, S. G., Kim, K. C., Namkung, J. H., Rho, B. J. and Song, K. K. 2001, "Spray Transport and Atomization in two phase swirl atomizer", *Proceedings of ILASS-Asia 2001*, Oct. 11-13, Busan, Korea

Lee, S. G. and Rho, B. J., 2000, "Atomization Characteristics in Pneumatic Counterflowing Internal Mixing Nozzle," *KSME International Journal*, Vol. 14, No. 10, pp. 1131~1142.

Lee, S. G., Rho, B, J. and Song, K. K., 2001, "Turbulent Disintegration Characteristics in Twin Fluid Counter Flowing Atomizer." *39th ALAA Aerospace and Sciences Meeting and Exhibit, AIAA 2001-1047*, Jan. 8-11, 2001, Reno Nevada, U. S. A

Mansour, A. and Cgigier, N., 1990, "Disintegration of Liquid sheets," *Phys. Fluids A.*, pp. 706~719.

Mullinger, P. J., 1974, "The Design and Performance of Internal Mixing Multijet Twin Fluid Atomizers," *Journal of the Institute of Fuel*, pp. 251~261.